

Lipophilic pro-oligonucleotides are rapidly and efficiently internalized in HeLa cells

Eric Vivès¹, Christelle Dell'Aquila, Jean-Charles Bologna, François Morvan, Bernard Rayner and Jean-Louis Imbach*

Laboratoire de Chimie Bio-Organique, UMR 5625 CNRS-UM II, Université Montpellier II, Place Eugène Bataillon, 34095 Montpellier Cedex 5, France and ¹Institut de Génétique Moléculaire de Montpellier, UMR 5535 CNRS, Université Montpellier II, 1919, Route de Mende, BP 5051, 34293 Montpellier Cedex 5, France

Received June 17, 1999; Revised and Accepted August 30, 1999

ABSTRACT

Model *t*-Bu-SATE pro-dodecathymidines labeled with fluorescein and exhibiting various lipophilicities were evaluated for their uptake by cells in culture. Pro-oligonucleotides with appropriate lipophilicity were found to permeate across the HeLa cell membrane much more extensively than the control phosphorothioate oligo or than the hydrophilic pro-oligos. Fluorescence patterns of internalization were consistent with a diffusion mechanism resulting in the appearance of a uniform cytoplasmic distribution and nuclear accumulation, as confirmed by confocal microscopy.

INTRODUCTION

It is well established that the potential application of antisense oligonucleotides is mainly hampered by their instability in biological fluids and poor cell penetration (for a general discussion see ref. 1 and other related chapters in the book). These hurdles are related to their polyanionic structure and could be overcome by using the pro-drug approach (2). In this respect, we have recently shown that chemical derivatization of the internucleoside linkages with enzymolabile SATE (*S*-acetylthioethyl) protecting groups converts the parent oligonucleotides to neutral phosphotriester pro-drugs (3). Such pro-oligonucleotides, incorporating either methyl-SATE (*S*-acetylthioethyl) or *t*-butyl-SATE (*S*-pivaloylthioethyl) protecting groups, have been shown to resist enzymatic degradation by nucleases and to be selectively deprotected in cell extracts (as a model of the intracellular medium) (3,4).

We further expected that the lower charge density of such pro-oligos could result in increased cellular uptake. However, neutral SATE pro-oligos are highly lipophilic and hence hardly soluble in aqueous media. Therefore, approaches to selectively introduce some negative charges have been developed (4–6); the corresponding pro-oligos were 5'-labeled with fluorescein.

We report in this paper that such model (dT)₁₂ *t*-Bu-SATE pro-oligos present an increase in cellular permeation as compared to the parent oligo. More precisely, it seems that a correlation exists between uptake efficacy and the overall lipophilicity of the pro-oligo.

MATERIALS AND METHODS

Chemicals

All commercial chemicals were reagent grade and were used without further purification except where otherwise stated. DNA synthesis reagents, except oxidizers, were from Perseptive Biosystems Ltd (Voisins le Bretonneux, France). Anhydrous *t*-butyl hydroperoxide (3 M in toluene) was from Fluka and was diluted with anhydrous methylene chloride (Aldrich). 3*H*-1,2-Benzodithiole-3-one-1,1-dioxide (Beaucage's reagent) was a gift from Isis Pharmaceuticals (Carlsbad, CA).

Oligonucleotide synthesis

Pro-oligos were synthesized on an ABI synthesizer model 381 DNA using either *o*-methyl benzyl phosphoramidite (5; C.Dell'Aquila *et al.*; submitted for publication) or *H*-phosphonate (6), 5'-Dmtr-thymidine and *t*-butyl SATE phosphoramidite thymidine (3). Fluorescein labeling was performed using the carboxyfluorescein phosphoramidite derivative (Fig. 1) (C.Dell'Aquila *et al.*, submitted for publication). The pro-oligos were purified by HPLC and characterized by mass analysis.

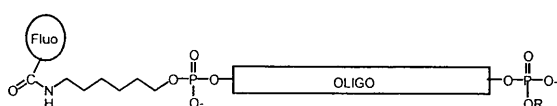
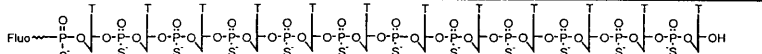
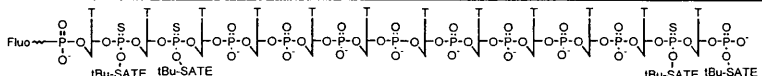
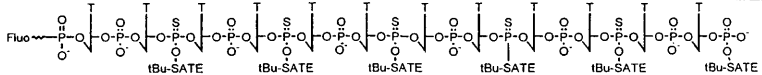
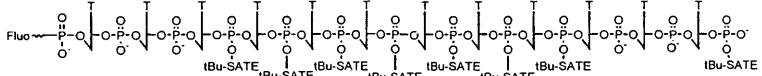
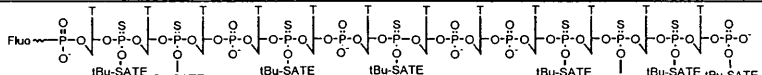
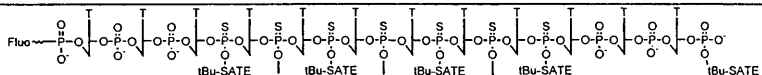
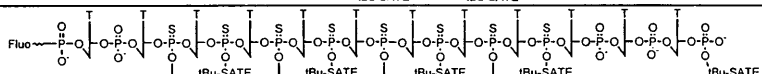
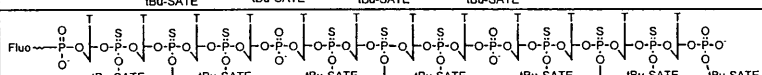
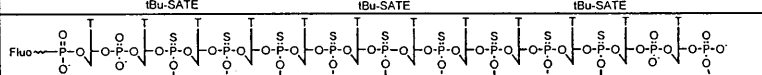
Analysis

High performance liquid chromatography (HPLC) analyses were performed on a Waters-Millipore instrument equipped with a Model 600E solvent delivery system, a Model U6K injector and a Model 486 UV detector. A reverse phase C₁₈ Nucleosil (5 μm) column (150 × 4.6 mm; Macherey-Nagel, Germany) was used at a flow rate of 1 ml min⁻¹. The retention time of each pro-oligo was determined using the following conditions: isocratic 50 mM triethyl ammonium acetate pH 7.0 for 7 min; a gradient of 0–80% acetonitrile over 74 min in the same buffer.

MALDI-TOF mass spectra were recorded on a Voyager mass spectrometer (Perseptive Biosystems, Framingham, MA) equipped with a nitrogen laser. One microliter of pro-oligo sample (0.1 A_{260 nm} in 100 μl water:acetonitrile, 50:50 v/v) was exchanged on ammonium Dowex 50W X8 resin before addition of 10 μl of a saturated solution of 2,4,6-trihydroxyacetophenone in acetonitrile:water (1:1 v/v) and 1 μl of ammonium citrate (pH 9.4, 100 mM in water). This mixture was placed on a plate and dried at ambient temperature and pressure.

*To whom correspondence should be addressed. Tel: +33 4 67 41 25 30; Fax: +33 4 67 04 20 29; Email: imbach@univ-montp2.fr

Table 1. Structure of the fluorescein-labeled *t*-Bu-SATE pro-oligos 1–9

		RT (min.)	# of charge s
1		37.0	12
2		49.5	10
3		51.4	8
4		59.0	6
5		63.0	6
6		69.5	6
7		75.0	5
8		78.0	4
9		80.0	4

Cells and cell culture

HeLa GH cells (derived from HeLa 229) and CCL 39 Chinese hamster cells were cultured on 90 mm plates as exponentially growing subconfluent monolayers in RPMI 1640 medium or Dulbecco's modified Eagle's medium, respectively, supplemented with 2 mM glutamine and 10% (v/v) fetal calf serum. To test the different compounds on cells, cell monolayers were treated with a non-enzymatic cell dissociation medium (Sigma), and 15 000 cells/well were plated on 8-well Lab-Teck plates (Nunc Inc., Naperville, IL) and cultured overnight. The culture medium was discarded and cells were washed once with phosphate-buffered saline (PBS) pH 7.4, before a 30 min preincubation step in Opti-MEM medium (Gibco, Cergy-Pontoise, France). Preincubation Opti-MEM medium was discarded and the cells were incubated with the pro-oligo solution.

Fluorescence microscopy

Stock solutions of fluorescein-labeled *t*-Bu-SATE oligonucleotides and control oligonucleotide were dissolved in TE buffer (10 mM Tris-HCl, 1 mM EDTA, pH 8) at a concentration of 100 μ M and stored at -20°C until further use. Pro-oligo solutions were prepared just before experiments at the appropriate concentration from stock solutions in 10 μ l of TE completed up to 100 μ l with Opti-MEM. After removal of the preincubation

medium, the pro-oligo solution in Opti-MEM was added and cells were incubated at 37°C , 5% CO_2 for various times. Subsequently, the pro-oligo solution was discarded, cells were washed three times for 5 min with PBS at room temperature and fixed in most cases for 5 min in 3.7% (v/v) formaldehyde solution in PBS at room temperature. However, other fixation procedures, such as fixation in ethanol:acetic acid (95:5 v/v) for 5 min at -20°C or with methanol for 6 min at -20°C , were also performed. Moreover, internalization was also evaluated without any fixation, but following the same washing protocol. After fixation, cells were washed three more times for 3 min with PBS before incubation at room temperature for 2 min with Hoescht 33258 (50 ng/ml) solution in PBS for nuclei staining. After three additional washes with PBS, cells were then mounted directly with VectashieldTM. The distribution and the level of fluorescence was observed on a Zeiss Axiophot fluorescence microscope equipped with a 100 W mercury lamp as previously described (7). Images were captured with a slow scan charge-coupled device camera (κ CF 8/1 DX) and analyzed using Adobe Photoshop v.5.0 software.

RESULTS AND DISCUSSION

Table 1 presents the evaluated 5'-fluorescein-(dT)₁₂ pro-oligos containing between 4 and 10 *t*-Bu SATE protecting groups. As

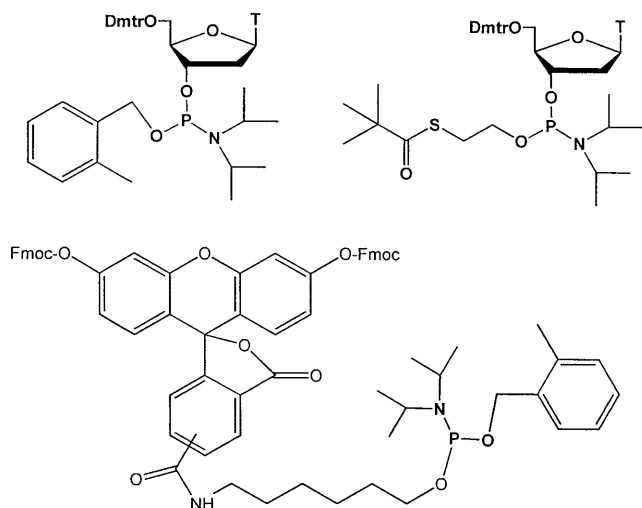


Figure 1. Building blocks used for the synthesis of fluorescein-labeled pro-oligos 1–9.

these compounds (except **1**) contain SATE phosphotriesters their solid phase synthesis must preclude any basic conditions, hence the use of a photolabile linker (**8**) and our limitation to model dodecathymidylates.

Introduction of phosphodiester linkages in predetermined positions was performed using two selective methods. Compounds **2–6** were synthesized using phosphoramidite chemistry with *t*-Bu-SATE and *o*-methylbenzyl building blocks (Fig. 1). Negative charges were created upon iodine treatment of the *o*-methylbenzyl phosphite protecting groups (**5**). Pro-oligos **6–9** were obtained using both the phosphoramidite and *H*-phosphonate chemistries for SATE phosphotriester and phosphodiester linkages, respectively (**6**). Control oligo **1** was synthesized using standard *H*-phosphonate chemistry with a final sulfurization by treatment with elemental sulfur (**9**). Fluorescein was introduced at the 5'-end of the pro-oligos (**1–9**) using a phosphoramidite derivative of hexamethylene 4,5-carboxy fluorescein with Fmoc protecting groups on phenolic functions and an *o*-methylbenzyl protecting group on the phosphorus atom (Fig. 1).

The relative retention times (RT) for each oligo derivative, a reflection of their relative hydrophobicity (**10**), were determined using a C₁₈ reverse phase HPLC system (Table 1). It is noteworthy that the retention time of the pro-oligos increases with the number of SATE groups and concomitant diminution of the negative charge number. In addition, compounds **4** and **6** (with seven SATE groups) only differ by the replacement of six oxo by six thiono groups, which thus gives rise to an important increase in hydrophobicity.

Cellular uptake of the pro-oligos

The cellular uptake of the different fluorescein-labeled pro-oligos synthesized in this study was estimated directly by fluorescence microscopy. The incubation of these pro-oligos was performed without addition of any transfecting reagent. However, to

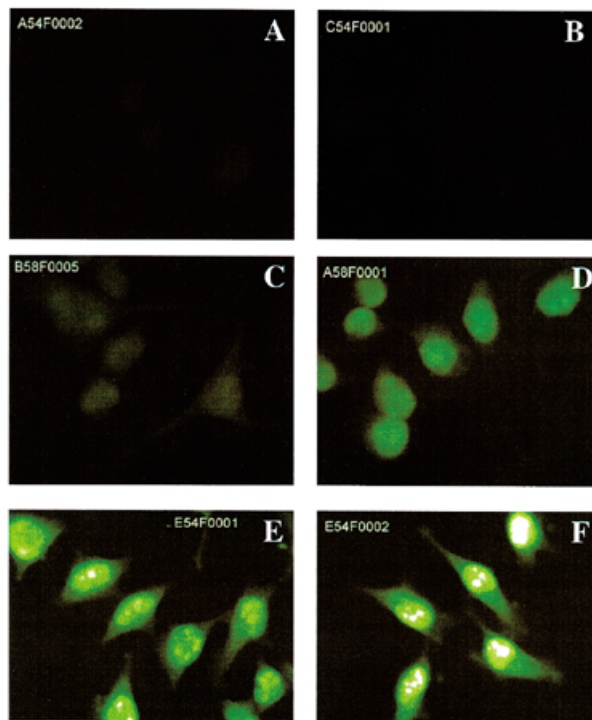


Figure 2. Incubation of SATE pro-oligos **2–6** with HeLa cells. Fluorescence microscopy of HeLa cells incubated with an equivalent dose (10 μ M) of each SATE pro-oligonucleotide for 1 h at 37°C. (A) Compound **2**; (B) compound **3**; (C) compound **4**; (D) compound **5**; (E and F) compound **6**. Images were acquired with the same camera settings for all pro-oligos.

circumvent or to limit extracellular stability problems of the different compounds, incubations were performed in serum-free medium, namely Opti-MEM. Since pro-oligos **2–9** were constituted with phosphodiester linkages which could be hydrolyzed by endonucleases, incubation experiments were carried out in serum-free medium to exclude any problem of degradation that could lead to misinterpretation. Under both identical incubation procedures (duration of the incubation and extracellular dose of compounds **1–6**) and camera acquisition settings, the behavior of the different pro-oligos appeared to be significantly different. First, the parent oligonucleotide in the phosphorothioate series without a SATE group (compound **1**) was used as a control oligonucleotide. When incubated with HeLa cells for up to 3 h at an extracellular dose of 10 μ M, fluorescein-labeled compound **1** was only very faintly detected (data not shown). This cell line was also incubated with 10 μ M carboxyfluorescein without showing any fluorescent signal. The fluorescein moiety was found to be stable in total cell extract by mass spectrum analysis (MALDI-TOF). Pro-oligos **2–6** showed a different ability for uptake when incubated with HeLa cells for 1 h at a dose of 10 μ M (Fig. 2). When compared under identical camera parameter settings, a variation in the intensity of fluorescence entrapped within cells was obvious, depending on the pro-oligo. In summary three main magnitudes

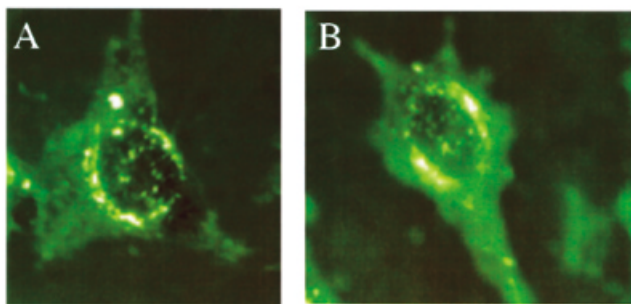


Figure 3. Incubation of SATE pro-oligo **9** (10 μ M for 1 h at 37°C) with HeLa cells. (A and B) Two different cells with characteristic perinuclear labeling.

of fluorescence could be observed among this series of pro-oligos. Pro-oligos **2** and **3** induced a very low cellular labeling (Fig. 2A and B, respectively), but, as low as the signal was, it could be significant when compared to the control oligonucleotide. For instance, compounds **2** and **3** required a 10-fold increase in the acquisition time to induce a visible signal (data not shown). However, to maintain the relative intensity between these compounds as observed under fluorescence microscopy, Figure 2 is set to show all the oligonucleotides with identical incubation and acquisition parameters. Pro-oligos **4** and **5** induced a stronger signal which could be easily detected at that dose and under our camera settings (Fig. 2C and D, respectively). However, pro-oligo **6** showed the strongest signal among this first series of pro-oligos (Fig. 2E and F). The internalization of pro-oligo **6** could be detected unambiguously at lower doses, down to 100 nM (data not shown).

Based on the relative lipophilicity of oligos **1–6** (expressed as their RT in Table 1), a relationship between uptake and lipophilicity thus appeared to be a key factor in explaining the reported pro-oligo internalization. As the most lipophilic pro-oligo, oligo **6** (among compounds **1–6**), was much more efficiently taken up by cells, a second set of more lipophilic pro-oligos, oligos **7–9** (see Table 1 for pro-oligo structures), was further evaluated under identical conditions as described above. When uptake of this new series of pro-oligos **7–9** was compared to pro-oligo **6** uptake, the fluorescence signal associated with the cells appeared to be slightly stronger for pro-oligos **7** and **8** (data not shown). However, the fluorescent signal for the most hydrophobic pro-oligo, oligo **9**, showed a very different pattern (Fig. 3A and B); first, the overall fluorescent signal was remarkably reduced in terms of intracellular fluorescence intensity and, second, general cellular labeling was very punctated, mainly around the cell nucleus, thus suggesting entrapment of this pro-oligo in the endosome pathway. Moreover, significant fluorescent punctation was also visible at the cellular membrane level (data not shown), although the solubility of this latter compound was assessed independently in the incubation medium.

The uptake of these pro-oligos was also evaluated in CCL 39 cells without exhibiting a different pattern in terms of fluorescent intensity and cellular distribution (data not shown).

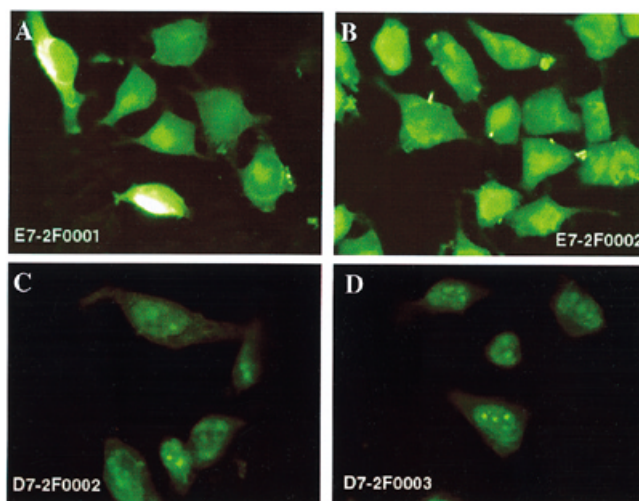


Figure 4. Incubation of SATE pro-oligos **6** (10 μ M for 1 h) with HeLa cells at 37 (A and B) and 4°C (C and D).

Additionally, the toxicity of such pro-oligos was also evaluated by performing a MTT test (7) for 24 h at the doses used in this study (1 and 10 μ M). Despite the much longer incubation time for this toxicity assay compared to our standard incubation time (from 1 to 3 h), cell viability was not affected.

It therefore seemed obvious that the overall lipophilicity of these pro-oligos was a key factor in their uptake. However, preliminary data with pro-oligo **6** in the presence of 10% serum seemed to indicate a decrease in uptake, as observed with cationic lipid-phosphorothioate oligonucleotide complexes (11).

Temperature effect on pro-oligo uptake

It is commonly accepted that performing incubation assays with cells at low temperature (i.e. 4°C) with soluble extracellular compounds dramatically reduced the endocytosis pathway, which could eventually induce their cellular uptake. To further investigate the way in which SATE pro-oligos enter the cell, incubation of cells with compound **6** was performed at 4°C. Basically, cells were cooled to 4°C for 1 h before being incubated with pre-cooled solutions of pro-oligos for 1 h. Rinsing and early fixation were also performed at 4°C before mounting the slides for fluorescent microscopy observation. Despite these incubation procedures, substantial detection of intracellular fluorescence could be detected without variation in its cellular sublocalization. A first quantification of the internalized fluorescence indicated that >50% of the signal could still be detected under these conditions (Fig. 4), thus excluding uptake of the pro-oligo through the endosome pathway. The hydrophobic properties of these pro-oligos could of course suggest a direct membrane fusion process to explain their uptake. Along these lines, the observed reduction in uptake at low temperature could reflect a relative loss of the membrane fusion process occurring once the pro-oligos were entrapped in endosome vesicles under standard incubation conditions.

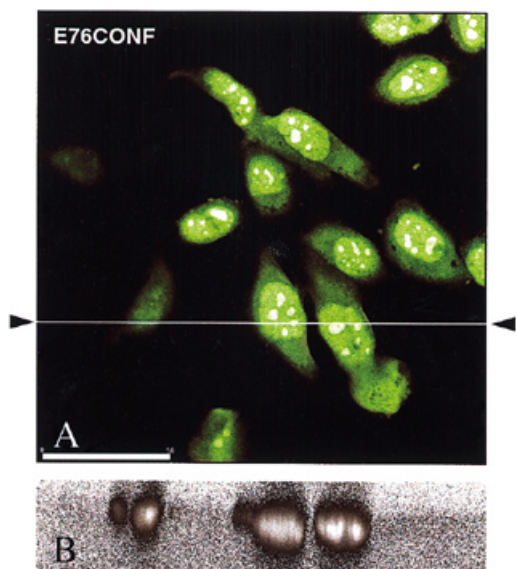


Figure 5. Confocal microscopy of the SATE pro-oligos on HeLa cells. (A) Confocal acquisitions of HeLa cells incubated with $1 \mu\text{M}$ of **6** for 1 h at 37°C . Confocal acquisition with a z step of $0.1 \mu\text{m}$ was performed. A single confocal view corresponding to a medium z step. Images were acquired with the Laserssharp 1024 software and processing system. Images were scanned at 1024×1024 pixels resolution. (B) The cumulative lateral projection (x - z section) of the confocal views corresponding to the line shown by arrows in (A). The scale bar in (A) indicates $50 \mu\text{m}$.

Subcellular localization of the pro-oligos and confocal microscopy

When cells are incubated with non-permeant molecules such as fluorescein-labeled oligonucleotides, a punctated area corresponding to the endosome vesicles is usually observed. It is also accepted and has been demonstrated that once an oligonucleotide reaches the cytosol, it should then migrate to the nucleus (12). In this study no particular pattern concerning the intracellular route and/or distribution of the pro-oligos synthesized here was observed. In no cases was specific labeling of subcellular structures related to the endosome system, such as perinuclear vesicles, observed under our experimental conditions. Most of the compounds we used showed their associated fluorescence to be diffuse in the whole cell without any particular cytoplasmic localization in general, suggesting that pro-oligo uptake could bypass the endosome pathway.

Moreover, a large majority of cells incubated with pro-oligo **6** showed fluorescence mainly concentrated in the nucleus, with nucleolar accumulation. To confirm the intracellular localization of pro-oligo **6**, confocal microscopy was performed on HeLa cells incubated with $1 \mu\text{M}$ pro-oligo **6** for 1 h (Fig. 5). A full series of optical sections with a z step of $0.1 \mu\text{m}$ was collected. Figure 5A shows a single confocal view corresponding to a medium z step. Figure 5B is a cumulative lateral projection of the confocal views corresponding to the line shown by arrows in Figure 5A. Both views show the

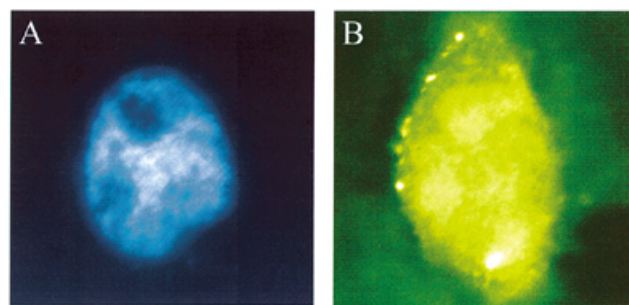


Figure 6. (A) The cell nucleus stained with Hoechst's reagent. Darker areas correspond to nucleolei. (B) Diffuse labeling of the cell with faint nucleolar accumulation.

intracellular and, more particularly, the intranucleolar accumulation of pro-oligo **6**. This nucleolar accumulation could also be noted in some cells for other compounds, such as pro-oligos **7** and **8**. However, further studies should be performed to reconcile the apparent differences occurring in the final compartmentalization of these pro-oligos.

Fluorescence microscopy after several fixation procedures

An artefactual effect in cellular internalization and/or in sublocalization due to the fixation procedure is often suggested when performing this kind of study (13). To investigate such a possibility, various fixation procedures among those most employed were performed in addition to the fixation with formaldehyde used in the above experiments. These included fixation with ethanol:acetic acid (95:5 v/v) and with methanol, both at -20°C and for 5 or 6 min, respectively. No variation in the rate of internalization of the different pro-oligos or in their sublocalization was observed. Additionally, pro-oligo **6** uptake was also determined in living cells without any fixation at $1 \mu\text{M}$ after a 1 h incubation (Fig. 6). An identical propensity for pro-oligo **6** to enter the cells was observed as diffuse labeling. A faint accumulation of the pro-oligo was noticeable at the nucleolar level (Fig. 6). Similar experiments with pro-oligos **7–9** at $10 \mu\text{M}$ showed intracellular fluorescence signals comparable to those observed after cell fixation.

Time course of internalization

To investigate a discrete sublocalization of the pro-oligo during uptake, such as membrane- or vesicle-associated fluorescence, a time course experiment was performed. Basically, HeLa cells were incubated with $1 \mu\text{M}$ pro-oligo **6** for 2, 5, 10, 15, 30, 45 and 60 min. Cellular fluorescence could be unambiguously detected after only 2 min incubation (data not shown). However, the signal appeared to reach a maximum level at 10 min. Shorter than that duration no fluorescence could be found associated with any cellular substructure, which favors the hypothesis of simple diffusion through the plasma membrane due to the lipophilicity of the *t*-Bu-SATE pro-oligo. Moreover, internalization of the pro-oligo appeared to be relatively fast.

CONCLUSION

The data reported in this paper demonstrate that, under our experimental conditions, model *t*-Bu-SATE (dT)₁₂ pro-oligos with an appropriate hydrophobicity are membrane diffusible compounds which are localized homogeneously in the cytoplasm and are accumulated in the nucleus. This high uptake is a necessary requirement for putative use of pro-oligos as pharmaceutical agents, provided that they can be selectively demasked intracellularly. Along this line, complementary experiments with pro-oligos bearing nuclease-resistant phosphorothioate diester linkages are in progress. It is hoped that specific pro-oligos able to selectively inhibit gene expression will be obtained in the future.

ACKNOWLEDGEMENTS

We are grateful to Pr Bernard Lebleu (IGM, Montpellier) for helpful discussions, to Nicole Lautrédou (CRIC, Montpellier) for performing confocal data acquisitions and to Ian Robbins (IGM, Montpellier) for proof-reading of the manuscript. This work was supported by grants from the Agence Nationale de Recherche sur le SIDA (ANRS) and from ISIS Pharmaceuticals. C.D. and G.T. thank the Association pour la Recherche contre le Cancer (ARC) and J.-C.B. thanks the Association pour le Développement et l'Enseignement et la Recherche (ADERLR) for the award of a research studentship.

REFERENCES

1. Crooke, R.M. (1998) In Crooke, S.T. (ed.), *Antisense Research and Application*. Springer-Verlag, Berlin, Germany, Vol. 131, pp. 103–140.
2. Krise, J.P. and Stella, V.J. (1996) *Adv. Drug Deliv. Rev.*, **19**, 287–310.
3. Tosquellas, G., Alvarez, K., Dell'Aquila, C., Morvan, F., Vasseur, J.J., Imbach, J.L. and Rayner, B. (1998) *Nucleic Acids Res.*, **26**, 2069–2074.
4. Tosquellas, G., Bologna, J.C., Morvan, F., Rayner, B. and Imbach, J.L. (1998) *Bioorg. Med. Chem. Lett.*, **8**, 2913–2918.
5. Caruthers, M.H., Kierzek, R. and Tang, J.Y. (1987) In Bruzik, K.S. and Stec, W.J. (eds), *Biophosphates and their Analogues. Synthesis, Structure, Metabolism and Activity*. Elsevier, Amsterdam, The Netherlands, pp. 3–21.
6. Bologna, J.-C., Morvan, F. and Imbach, J.-L. (1999) *Eur. J. Org. Chem.*, 2353–2358.
7. Vives, E., Brodin, P. and Lebleu, B. (1997) *J. Biol. Chem.*, **272**, 16010–16017.
8. Dell'Aquila, C., Imbach, J.L. and Rayner, B. (1997) *Tetrahedron Lett.*, **38**, 5289–5292.
9. Stein, C.A., Iversen, P.L., Subasinghe, C., Cohen, J.S., Stec, W.J. and Zon, G. (1990) *Anal. Biochem.*, **188**, 11–16.
10. Crooke, S.T., Graham, M.J., Zuckerman, J.E., Brooks, D., Conklin, B.S., Cummins, L.L., Greig, M.J., Guinosso, C.J., Kornbrust, D., Manoharan, M., Sasmor, H.M., Schleich, T., Tivel, K.L. and Griffey, R.H. (1996) *J. Pharmacol. Exp. Ther.*, **277**, 923–937.
11. Litzinger, D.C., Brown, J.M., Wala, I., Kaufman, S.A., Van, G.Y., Farrell, C.L. and Collins, D. (1996) *Biochim. Biophys. Acta*, **1281**, 139–149.
12. Leonetti, J.P., Mechti, N., Degols, G., Gagnor, C. and Lebleu, B. (1991) *Proc. Natl Acad. Sci. USA*, **88**, 2702–2706.
13. Pichon, C., Monsigny, M. and Roche, A.-C. (1999) *Antisense Nucleic Acid Drug Dev.*, **9**, 89–93.